

# Synchronization of Weakly Coupled Oscillators: Coupling, Delay and Topology

Enrique Mallada and A. Kevin Tang  
Cornell University, Ithaca, NY 14853

## Abstract

There are three key factors of a system of coupled oscillators that characterize the interaction among them: *coupling* (*how to affect*), *delay* (*when to affect*) and *topology* (*whom to affect*). For each of them, the existing work has mainly focused on special cases. With new angles and tools, this paper makes progress in relaxing some assumptions of these factors. There are three main results in this paper. First, by using results from algebraic graph theory, a sufficient condition is obtained which can be used to check equilibrium stability. This condition works for arbitrary topology. It generalizes existing results and also leads to the first sufficient condition on the coupling function with which the system is guaranteed to reach synchronization. Second, it is known that identical oscillators with  $\sin(\cdot)$  coupling functions are guaranteed to synchronize in phase on a complete graph. Using our results, we demonstrate that for many cases certain structures instead of exact shape of the coupling function such as symmetry and concavity are the keys for global synchronization. Finally, the effect of heterogenous delays is investigated. We develop a new framework by constructing a non-delayed phase model that approximates the original one in the continuum limit. We further derive how its stability properties depend on the delay distribution. In particular, we show that heterogeneity, i.e. wider delay distribution, can help reach in-phase synchronization.

## I. INTRODUCTION

The system of coupled oscillators has been widely studied in different disciplines ranging from biology [1], [2], [3], [4], [5] and chemistry [6], [7] to engineering [8], [9] and physics [10], [11]. The possible behavior of such a system can be complex. For example, the intrinsic symmetry of the network can produce multiple limit cycles or equilibria with relatively fixed phases (phase-locked trajectories) [12], which in many cases can be stable [13]. Also, the heterogeneity in the natural oscillation frequency can lead to incoherence [14] or even chaos [15].

One particular interesting question is whether the coupled oscillators will synchronize in phase in the long run. Besides its clear theoretical value, it also has rich applications in practice such as clock synchronization in distributed systems. There has been active research work regarding this question, see e.g., [16], [17], [18], [19].

In essence, there are three key factors of a system of coupled oscillators that characterize the interaction among oscillators: *coupling*, *delay* and *topology*. For each of them, the existing work has mainly focused on special

cases as explained below. In this paper, further research will be discussed on each of these three factors:

- Topology (*whom to affect*, Section IV-B): Current results are mainly restricted to complete graph or a ring topology for analytical tractability. We develop a graph based sufficient condition which can be used to check equilibrium stability for any topology. It also leads to the coupling function with which the system is guaranteed to reach synchronization.
- Coupling (*how to affect*, Section IV-C): The classical Kuramoto model [14] assumes a  $\sin()$  coupling function. Our study hints that certain symmetry and convexity structures are enough to guarantee global synchronization.
- Delay (*when to affect*, Section V). Existing work generally assumes zero delay among oscillators, which is clearly not satisfactory especially if the oscillating frequencies are high. We develop a new framework to study them by constructing a non-delayed phase model that is equivalent to the original one. Using this result, we show that wider delay distribution can help reach synchronization.

In this paper we study *weakly* coupled oscillators, which can be either pulse-coupled or phase-coupled. Although most of the results are presented for phase-coupled oscillators, they can be readily extended for pulse-coupled oscillators (see, e.g., [20], [21]). It is worth noticing that results in Section IV are independent of the strength of the coupling and therefore the weak coupling assumption is not necessary there.

The paper is organized as follows. After introducing the model and notation in Section II, we study three motivating examples in Section III. These examples provide basic intuition about the possible complex behavior of networks with coupled oscillators and therefore motivate further study. With some facts from algebraic graph theory and potential dynamics in section IV-A, we present the negative cut instability theorem in section IV-B1 to check whether an equilibrium is unstable. This then leads to Theorem 6 in section IV-B2 which identifies a class of coupling functions with which the system always synchronizes in phase. It is well known that the Kuramoto model produces global synchronization over a complete graph. In section IV-C, we demonstrate that a large class of coupling functions, in which the Kuramoto model is a special case, guarantee the instability of most of the limit cycles in a complete graph network. Section V is devoted to the discussion of the effect of delay. An equivalent non-delayed phase model is constructed whose coupling function is the convolution of the original coupling function and the delay distribution. Using this approach, it is shown that sometimes more heterogeneous delays among oscillators can help reach synchronization. We conclude the paper in Section VI.

## II. MODEL

In this section we describe two different models of coupled oscillators. Their difference arises in the way that the oscillators interact between each other, and their dynamics can be quite different. However, when the interactions are weak (weak coupling), both systems behave similarly and share the same approximation. This allows us to study them under a common framework.

Consider the set of  $N$  identical oscillators,  $\mathcal{N}$ , whose states can be represented by phase variables  $\theta_i \in \mathbb{S}^1$  for each oscillator  $i \in \mathcal{N}$ . In the absence of coupling, we have

$$\dot{\theta}_i = \omega, \quad \forall i \in \mathcal{N}.$$

Here,  $\mathbb{S}^1$  represents the unit circle, or equivalently the interval  $[0, 2\pi]$  with 0 and  $2\pi$  identified ( $0 \equiv 2\pi$ ), and  $\omega = \frac{2\pi}{T}$  denotes the natural frequency of the oscillation.

The state space of the whole system is the  $N$  dimensional torus  $\mathcal{T}^N$  which corresponds to the direct sum of  $N$  unit circles, i.e.  $\phi = (\phi_1, \dots, \phi_N)^T \in \mathcal{T}^N = \mathbb{S}_1^1 \oplus \dots \oplus \mathbb{S}_N^1$ .

### A. Pulse-coupled Oscillators

In the canonical model of pulse-coupled oscillators [21], an oscillator  $j \in \mathcal{N}$  sends out a pulse whenever it crosses zero ( $\theta_j = 0$ ). When oscillator  $i$  receives a pulse, it will change its position from  $\theta_i$  to  $\theta_i + \varepsilon \kappa_{ij}(\theta_i)$ . The function  $\kappa_{ij}$  represents how other oscillators' actions affect oscillator  $i$  and the scalar  $\varepsilon > 0$  is a measure of the coupling strength. These jumps can be modeled by a Dirac's delta function  $\delta$  satisfying  $\delta(t) = 0 \quad \forall t \neq 0$ ,  $\delta(0) = +\infty$ , and  $\int \delta(s) ds = 1$ . The coupled dynamics is represented by

$$\dot{\theta}_i(t) = \omega + \varepsilon \omega \sum_{j \in \mathcal{N}_i} \kappa_{ij}(\theta_i(t)) \delta(\theta_j(t - \eta_{ij})), \quad (1)$$

where  $\eta_{ij} > 0$  is the propagation delay between oscillators  $i$  and  $j$  ( $\eta_{ij} = \eta_{ji}$ ), and  $\mathcal{N}_i$  is the set of  $i$ 's neighbors. The factor of  $\omega$  in the sum is needed to keep the size of the jump within  $\varepsilon \kappa_{ij}(\theta_i)$ . This is because  $\theta_j(t)$  behaves like  $\omega t$  when crosses zero and therefore the jump produced by  $\delta(\theta_j(t))$  is of size  $\int \delta(\theta_j(t)) dt = \omega^{-1}$  [21].

This pulse-like interaction between oscillators was first introduced by Peskin [2] in 1975 as a model of the pacemaker cells of the heart, although the canonic form did not appear in the literature until 1999 [21]. The coupling function  $\kappa_{ij}$  is usually classified based on its sign; if  $\kappa_{ij} > 0$ , the coupling is **excitatory** and if  $\kappa_{ij} < 0$ , then it is **inhibitory** coupling. This classification is based on models of biological oscillatory networks, but is not sufficient even to characterize the system's qualitative behavior and usually a first order derivative conditions

is needed to obtain desired synchronization.

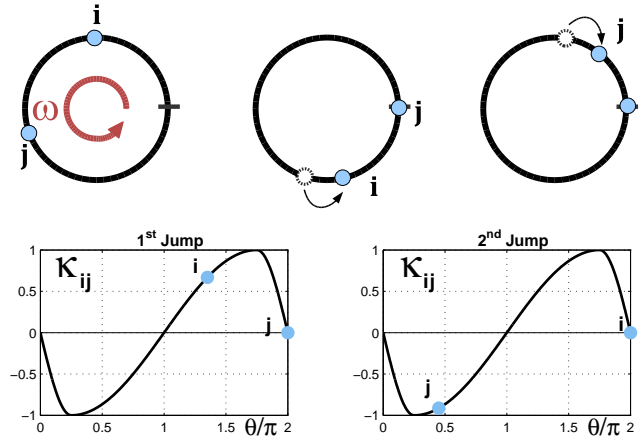


Fig. 1. **Pulse-coupled oscillators with attractive coupling.**

Here we introduce a different criterion that takes into account the qualitative behavior of the system. After one period, if the net effect of the mutual jumps brings a pair of oscillators closer, we call it **attractive** coupling. If the oscillators are brought further apart, it is considered to be **repulsive** coupling. The former can be achieved for instance if  $\kappa_{ij}(\theta) \leq 0$  for  $\theta \in [0, \pi)$  and  $\kappa_{ij}(\theta) \geq 0$  for  $\theta \in [\pi, 2\pi)$ . See Figure 1 for an illustration of an attractive coupling  $\kappa_{ij}$  and its effect on the relative phases.

In general, when the number of oscillators is large, there are several different limit cycles besides the in-phase synchronization and many of them can be stable [13]. Thus, predicting whether the system will reach in-phase synchronization is generally not an easy task. The problem was solved for the complete graph case by Mirollo and Strogatz in 1990 [22] by showing that if  $\kappa_{ij}(\theta)$  is strictly increasing (which resembles attractive coupling), then for almost every initial condition, the system can synchronize in phase in the long run.

The analysis in [22] strongly depends on the assumptions of complete graph and zero delay among oscillators. When the graph is no longer complete, each pulse receives a different firing pattern which makes the proof in [22] no longer valid. On the other hand, when delay among oscillators is introduced, which is necessary for many interesting cases in practice, the analysis becomes intractable. Even for the case of two oscillators, the number of possibilities to be considered is large [23], [24].

### B. Phase-coupled Oscillators

In the model of phase-coupled oscillators, the interaction between neighboring oscillators  $i$  and  $j \in \mathcal{N}_i$  is modeled by change of the oscillating speeds. Although in general the speed change can be a function of both

phases  $(\theta_i, \theta_j)$ , in many scenarios it reduces to a function of the phase differences  $f_{ij}(\phi_j(t - \eta_{ij}) - \phi_i(t))$ . Thus, since the net speed change of oscillator  $i$  amounts to the sum of the effects of its neighbors, the full dynamics is described by

$$\dot{\phi}_i(t) = \omega + \varepsilon \sum_{j \in \mathcal{N}_i} f_{ij}(\phi_j(t - \eta_{ij}) - \phi_i(t)). \quad (2)$$

The function  $f_{ij}$  is usually called coupling function, and as before  $\eta_{ij}$  represents delay and  $\mathcal{N}_i$  is the set of neighbors of  $i$ .

A similar definition for attractive and repulsive couplings can be done in this model. We say that the coupling function  $f_{ij}$  is attractive if, without delays, the change in speeds brings oscillators closer, and repulsive if they are brought apart. Figure 2 shows typical attractive and repulsive coupling functions where arrows represent the speed change produced by the other oscillator; if the pointing direction is counter clockwise, the oscillator speeds up, and otherwise it slows down.

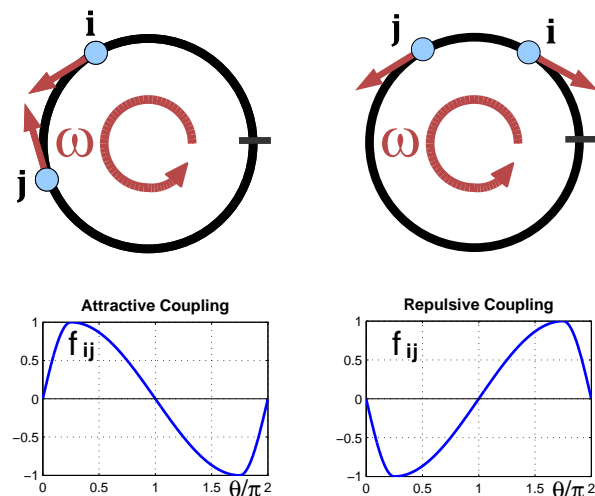


Fig. 2. **Phase-coupled oscillators with attractive and repulsive coupling.**

When  $f_{ij} = \frac{K}{N} \sin(\cdot)$  (attractive coupling), this model is known as the classical Kuramoto model [25]. Intensive research work has been conducted on this model, however convergence results are usually limited to cases with all to all coupling ( $\mathcal{N}_i = \mathcal{N} \setminus \{i\}$ , i.e., complete graph topology) and no delay ( $\eta_{ij} = 0$ ), see e.g. [19], or to some regions of the state space [26].

### C. Weak Coupling Approximation

Throughout this paper we assume that for both models the coupling strength is weak, i.e.  $1 \gg \varepsilon > 0$ . For pulse-coupled oscillators, this implies that the effect of the jumps originated by each neighbor can be approximated by their average [20]. For phase-coupled oscillators, it implies that to the first order  $\phi_i(t - \eta_{ij})$  is well approximated by  $\phi_i(t) - \omega\eta_{ij}$ .

The effect of these approximations allows us to completely capture the behavior of both models using the following equation where we assume that every oscillator has the same natural frequency  $\omega$

$$\dot{\phi}_i = \varepsilon \sum_{j \in \mathcal{N}_i} f_{ij}(\phi_j - \phi_i - \psi_{ij}). \quad (3)$$

For pulse-coupled oscillators, the coupling function is given by

$$f_{ij}(\theta) = \frac{\omega}{2\pi} \kappa_{ij}(-\theta), \quad (4)$$

and the phase lag  $\psi_{ij} = \omega\eta_{ij}$  represents the distance that oscillator  $i$ 's phase can travel along the unit circle during the delay time  $\eta_{ij}$ . Equation (4) also shows that the attractive/repulsive coupling classification of both models are in fact equivalent, since in order to produce the same effect  $\kappa_{ij}$  and  $f_{ij}$  should be mirrored, as illustrated in Figure 1 and Figure 2.

Equation (3) captures the relative change of the phases and therefore any solution to (3) can be immediately translated to either (1) or (2) by adding  $\omega t$ . For example, if  $\phi^*$  is an equilibrium of (3), by adding  $\omega t$ , we obtain a limit cycle in the previous models.

From now on we will concentrate on (3) with the understanding that any convergence result derived will be immediately true for the original models. We are interested in the attracting properties of phase-locked invariant orbits within  $\mathcal{T}^N$ , which can be represented by

$$\phi(t) = \omega^* t \mathbf{1}_N + \phi^*,$$

where  $\mathbf{1}_N = (1, \dots, 1)^T \in \mathcal{T}^N$ , and  $\phi^*$  and  $\omega^*$  are solutions to

$$\omega^* = \varepsilon \sum_{j \in \mathcal{N}_i} f_{ij}(\phi_j^* - \phi_i^* - \psi_{ij}), \quad \forall i. \quad (5)$$

Whenever the system reaches one of these orbits, we say that it is synchronized or phase-locked. If furthermore, all the elements of  $\phi^*$  are equal, we say the system is synchronized **in-phase** or that it is **in-phase** locked. It is easy to check that for a given equilibrium  $\phi^*$  of (3), any solution of the form  $\phi^* + \lambda \mathbf{1}_N$ , with  $\lambda \in \mathbb{R}$ , is also an

equilibrium that identifies the same limit cycle. Therefore, two equilibria  $\phi^{1,*}$  and  $\phi^{2,*}$  will be considered to be equivalent, if both identifies the same orbit, or equivalently, if both belongs to the same set of equilibria

$$E_{\phi^*} := \{\phi \in \mathcal{T}^N \mid \phi = \phi^* + \lambda \mathbf{1}_N, \lambda \in \mathbb{R}\}.$$

### III. MOTIVATING EXAMPLES

In order to gain insight on the complexity of this problem, and its dependence on the shape of  $f_{ij}$ , the network topology and delay, we present three examples.

**Example 1 (Two Oscillators without delay)** *We first consider two connected oscillators without delay, and symmetric coupling, i.e.,  $\mathcal{N} = \{1, 2\}$ ,  $\psi_{ij} = 0$  and  $f_{ij} = f_{ji} = f$ . Let  $f$  has a shape as in Figure 3 with  $f(0) = f(\pi) = 0$ . In this case (3) reduces to*

$$\dot{\phi}_i = \varepsilon f(\phi_j - \phi_i), \quad i, j \in \{1, 2\}, \quad j \neq i. \quad (6)$$

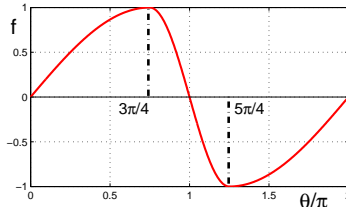


Fig. 3. Plot of function  $f$

Equation (6) has only two equilibria sets,  $E_{\phi_0^*}$  and  $E_{\phi_\pi^*}$ ; one in-phase identified by  $\phi_0^* = \mathbf{1}_N = (1, 1)^T$  and another in anti-phase identified by  $\phi_\pi^* = (0, \pi)^T$ . Also, because  $f(\theta) \geq 0$  for  $\theta \in [0, \pi]$  and  $f(\theta) \leq 0$  for  $\theta \in [\pi, 2\pi]$ , the coupling is **attractive** and thus unless the initial conditions belong to  $E_{\phi_\pi^*}$  both oscillators will always converge to  $E_{\phi_0^*}$  and thus synchronize in-phase.

However, this implies that Theorem 2 of [18] cannot hold, i.e. the in-phase equilibria set  $E_{\phi_0^*}$  is **not** globally asymptotically stable, since there is a set of initial conditions that do not converge to it. Furthermore, the Lyapunov function used in [18],  $|\phi|^2$ , does not work in the whole the state space. This can be readily verified in Figure 4(b), where  $|\phi(t)|^2$  can increase along trajectories even when the system synchronizes in-phase.

The preceding example is still simple in the sense that the anti-phase equilibria set  $E_{\phi_\pi^*}$  is unstable (as it is shown in Section IV-B1). However, when  $N > 2$ , new **stable** orbits  $E_{\phi^*}$  can appear as we show in the next example.

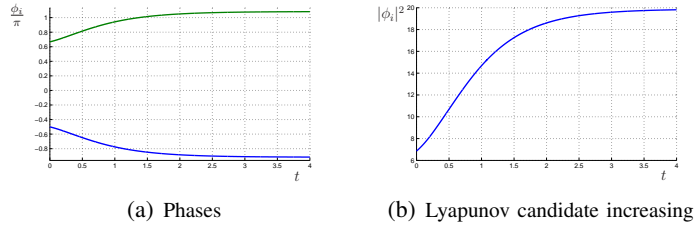


Fig. 4. A counter example for the Lyapunov function in [18]

**Example 2 (Three oscillators without delay)** Consider now three oscillators coupled all to all with the same function  $f$  as before and zero delay. Again, since  $f$  is odd, each phase locked solution of (5) must be an equilibrium (see Corollary 2.2 of [16]). However, due to network symmetry, a new **stable**  $E_{\phi^*}$  appears, with  $\phi^* = (-\frac{2\pi}{3}, 0, \frac{2\pi}{3})^T$ . Figure 5 illustrates it by showing the trajectories starting close to the set eventually converge to it, which suggests that the equilibrium set  $E_{\phi^*}$  is stable. This example hints that the problem can be very complex. Since as  $N$  grows, the number of sets  $E_{\phi^*}$  can explode and become difficult to locate for an arbitrary graph.

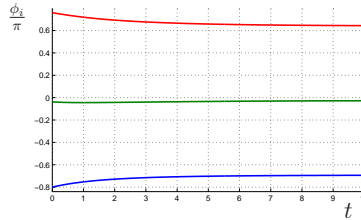


Fig. 5. A stable non-in-phase equilibrium in Example 2

**Example 3 (Two oscillators with delay)** Finally, suppose that there are two oscillators with coupling function  $H(\phi_j - \phi_i - \psi_{ij}) = K \sin(\phi_j - \phi_i - \psi_{ij})$ , i.e., the classical Kuramoto model [14]. Then (3) becomes

$$\dot{\phi}_i = \omega + \varepsilon K \sin(\phi_j - \phi_i - \psi) \quad i, j \in \{1, 2\}, j \neq i. \quad (7)$$

In the absence of delays ( $\psi = 0$ ) and for  $K > 0$  the scenario is identical to Example 1 and thus the coupling is **attractive**. Similarly, if  $K < 0$ , then the coupling is **repulsive** and the oscillators will move towards the anti-phase state unless they start in phase. Therefore, when there is no delay, one would tend to use  $K > 0$  in order to synchronize in-phase.

What is interesting here is the effect of the delay. For instance, when  $\psi_{ij} = \pi$ , a simple change of variable



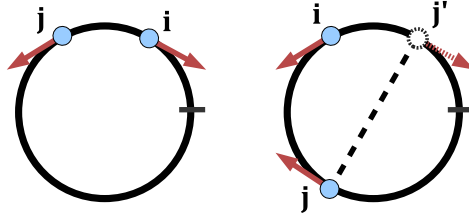


Fig. 6. **Repulsive coupling without delay vs. Repulsive coupling with delay of  $\pi$**

$\bar{\phi}_1 = \phi_1$ ,  $\bar{\phi}_2 = \phi_2 - \pi$  transforms (6) into

$$\dot{\bar{\phi}}_i = \omega + \varepsilon K \sin(\bar{\phi}_j - \bar{\phi}_i) \quad i, j \in \{1, 2\}, j \neq i.$$

Then from the previous discussion, by using attractive coupling ( $K > 0$ ) the system will tend to align  $\bar{\phi}_1$  with  $\bar{\phi}_2$ . However, this implies that the phase difference between  $\phi_1$  and  $\phi_2$  is  $\pi$ . On the other hand, when repulsive coupling ( $K < 0$ ) is used the  $\bar{\phi}_i$  variables reach the anti-phase configuration, which produces in turn in-phase synchronization for the original system.

The intuition behind this behavior is that performing repulsive actions over another oscillator whose phase is within  $\pi$  from where it is supposed to be has the net effect of bringing both oscillators closer instead of further apart. See Figure 6 for an illustration of this effect.

#### IV. EFFECT OF TOPOLOGY AND COUPLING

In this section we concentrate on the class of coupling function  $f_{ij}$  with the following characteristics:

**Assumption 1** *Properties of  $f_{ij}$ :*

- (a) *Symmetric coupling:*  $f_{ij} = f_{ji} \forall ij$ .
- (b) *Odd:*  $f_{ij}(-\theta) = -f_{ij}(\theta)$ .
- (c)  $C^1$ :  $f_{ij}$  is continuously differentiable.

Throughout this section we assume that there are no delay within the network, i.e.  $\psi_{ij} = 0 \forall ij \in E(G)$ . Thus, (3) reduces to

$$\dot{\phi}_i = \varepsilon \sum_{j \in \mathcal{N}_i} f_{ij}(\phi_j - \phi_i). \quad (8)$$

In the rest of this section we progressively show how Assumption 1 with some extra conditions on  $f_{ij}$  guarantees in-phase synchronization for arbitrary graph. Since we know that the network can have many other phase-locked

trajectories besides the in-phase one, our target is an **almost global stability** result [27], meaning that the set of initial conditions that does not eventually lock in-phase has zero measure. Latter we show how most of the phase-locked solution that appear on a complete graph are unstable under some general conditions on the structure of the coupling function.

### A. Preliminaries

We now introduce some prerequisites used in our later analysis together with some straightforward generalization of existing results.

1) *Algebraic Graph Theory* : We start by reviewing basic definitions and properties from graph theory [28], [29] that are used in the paper. Let  $G$  be the connectivity graph that describes the coupling configuration. Each graph is composed by two sets,  $V(G)$  and  $E(G) \subset V(G) \times V(G)$ , which are called vertex set and edge set, respectively. Each individual vertex is represented by  $i$  or  $j$ , and each edge by either  $e$  or the pair  $ij$ . If the graph is undirected, then  $ij$  and  $ji$  represent the same edge. Using this new framework,  $\mathcal{N} = V(G)$  and  $\mathcal{N}_i$  can be compactly defined as  $\mathcal{N}_i = \{j \in V(G) | ij \in E(G)\}$ .

An undirected graph  $G$  can be directed by giving a specific orientation  $\sigma$  to the elements in the set  $E(G)$ . That is, for any given edge  $e \in E(G)$ , we designate one of the vertices to be the *head* and the other to be the *tail*. The outcome of this operation is a directed graph  $G^\sigma$ , induced by  $G$ , where  $V(G) = V(G^\sigma)$  and for any  $ij \in E(G)$ , either  $ij \in E(G^\sigma)$  or  $ji \in E(G^\sigma)$ , but not both. We also attach to the convention that if  $e = ij \in E(G^\sigma)$  then  $i$  is the tail of  $e$  and  $j$  is its head.

**Remark 1** *Although all definitions described from now on implicitly require the graph to be oriented, the properties used in this paper are independent of a particular orientation  $\sigma$ . We therefore drop the superscript  $\sigma$  from  $G^\sigma$  with the understanding that  $G$  is now an induced directed graph with some fixed, but arbitrarily chosen, orientation.*

Each set  $V(G)$  and  $E(G)$  can be associated with a vector space over the real field. The **vertex space**  $\mathcal{V}(G)$  is the space of functions that maps  $V(G)$  into  $\mathbb{R}^{|V(G)|}$ , and the **edge space**  $\mathcal{E}(G)$  is the analogous for  $E(G)$  and  $\mathbb{R}^{|E(G)|}$ .

An oriented cycle  $L$  of the *oriented* graph  $G$  consists of an ordered sequence of vertices  $i_1 i_2 i_3 \dots i_l$  where  $i_1 = i_l$ ,  $i_k \neq i_1$  appears only once for  $k \in \{2, 3, \dots, l-1\}$  and either  $i_k i_{k+1} \in E(G)$  or  $i_{k+1} i_k \in E(G)$ . Let  $E(L)$  denote the set of edges that are in  $L$ , if  $e = i_k i_{k+1} \in E(L)$ , we say that  $e$  is oriented as  $L$ . Each oriented

cycle  $L$  determines an element  $z_L \in \mathcal{E}(G)$  as follows:

$$z_L(e_i) = \begin{cases} 1 & \text{if } e \in E(L) \text{ is oriented as } L, \\ -1 & \text{if } e \in E(L) \text{ is not oriented as } L, \\ 0 & \text{if } e \notin E(L). \end{cases}$$

If we let  $\mathcal{L}(G)$  be the set of all cycles within  $G$ , then the subspace  $\mathcal{Z}(G)$  of  $\mathcal{E}(G)$  spanned by all the vectors  $\{z_L\}_{L \in \mathcal{L}(G)}$ ,

$$\mathcal{Z}(G) := \text{span}\{z_L\}_{L \in \mathcal{L}(G)}$$

is called the **cycle space**.

Now let  $P = (V^-, V^+)$  be a partition of the vertex set  $V(G)$  such that  $V(G) = V^- \cup V^+$  and  $V^- \cap V^+ = \emptyset$ . The cut  $C(P)$  associated with  $P$ , or equivalently  $C(V^-, V^+)$ , is defined as  $C(P) := \{ij \in E(G) \mid i \in V^-, j \in V^+, \text{ or viceversa.}\}$ . Again, each partition also determines a vector  $c_P \in \mathcal{E}(G)$ :

$$c_P(e) = \begin{cases} 1 & \text{if } e \text{ goes from } V^- \text{ to } V^+, \\ -1 & \text{if } e \text{ goes from } V^+ \text{ to } V^-, \\ 0 & \text{if } e \notin E(V^-, V^+). \end{cases}$$

Analogously, the space spanned by all vectors  $c_P$  is called the **cut space** and denoted by  $\mathcal{C}(G)$ . A basic property of  $\mathcal{C}(G)$  and  $\mathcal{Z}(G)$  is that they are orthogonal complement; i.e.  $\mathcal{C}(G) \oplus \mathcal{Z}(G) = \mathcal{E}(G)$  and  $\mathcal{C}(G) \perp \mathcal{Z}(G)$ .

There are several matrices associated with the oriented graph  $G$  that embed information about its topology. However, the one with most significance to this work is the *oriented incidence matrix*  $B \in \mathbb{R}^{|V(G)| \times |E(G)|}$  where

$$B(i, e) = \begin{cases} 1 & \text{if } i \text{ is the head of } e, \\ -1 & \text{if } i \text{ is the tail } e, \\ 0 & \text{otherwise.} \end{cases}$$

We now list some properties of  $B$  that are used in subsequent sections.

(a) The null-space of  $B$  is the cycle space  $\mathcal{Z}(G)$ .

$$\text{i.e. } Bz = 0 \iff z \in \mathcal{Z}(G).$$

(b) The range of  $B^T$  is the cut space  $\mathcal{C}(G)$ , i.e., if  $z \in \mathcal{E}(G)$  is equal to  $B^T x$  for some  $x \in \mathcal{V}(G)$ , then  $z \in \mathcal{C}(G)$ . Or in other words, the column vectors of  $B^T$  span  $\mathcal{C}(G)$ .

(c) If  $G$  is connected, then  $\ker(B^T) = \text{span}(\mathbf{1}_N)$ .

2) *Potential Dynamics* : In Assumption 1, although  $f_{ij}$  being  $C^1$  is standard in order to study local stability and sufficient to apply LaSalle's invariance principle [30], the symmetry and odd assumptions have a stronger effect on the dynamics. For example, under these assumptions the system (8) can be compactly rewritten in a vector form as

$$\dot{\phi} = -\varepsilon BF(B^T \phi) \quad (9)$$

where  $B$  is the adjacency matrix defined in Section IV-A1 and the map  $F : \mathcal{E}(G) \rightarrow \mathcal{E}(G)$  is

$$F(y) = (f_{ij}(y_{ij}))_{ij \in E(G)}.$$

This new representation has several properties. First, from the properties of  $B$  one can easily show that (5) can only hold with  $\omega^* = 0$  for arbitrary graphs [16] (since  $N\omega^* = \omega^* \mathbf{1}_N^T \mathbf{1}_N = -\varepsilon \mathbf{1}_N^T BF(B^T \phi) = 0$ ), which implies that every phase-locked solution is an equilibrium of (8) and that every limit cycle of the original system (3) can be represented by some  $E_\phi^*$  on (8).

Additionally, (9) makes evident the difference between two classes of  $E_{\phi^*}$ . In the first,  $\phi^*$  is an equilibrium because  $F(B^T \phi^*) = 0$  and therefore  $\dot{\phi} = -\varepsilon BF(B^T \phi^*) = -\varepsilon B0 = 0$ . However, in the second class  $F(B^T \phi^*) \neq 0$  but  $F(B^T \phi^*) = z \in \mathcal{Z}(G)$ , and therefore when  $F(B^T \phi^*)$  is multiplied by  $B$  we get  $\dot{\phi} = -\varepsilon BF(B^T \phi^*) = -\varepsilon Bz = 0$ .

However, the most interesting consequence of (9) comes from interpreting  $F(y)$  as the gradient of a potential function

$$W(y) = \sum_{ij \in E(G)} \int_0^{y_{ij}} f_{ij}(s) ds.$$

Then, by defining  $V(\phi) = (W \circ B^T)(\phi) = W(B^T \phi)$ , (9) becomes a gradient descent law for  $V(\phi)$ , i.e.,

$$\dot{\phi} = -\varepsilon BF(B^T \phi) = -\varepsilon B \nabla W(B^T \phi) = -\varepsilon \nabla V(\phi),$$

where in the last step above we used the property  $\nabla(W \circ B^T)(\phi) = B \nabla W(B^T \phi)$ . This makes  $V(\phi)$  a natural Lyapunov function candidate since

$$\dot{V}(\phi) = \langle \nabla V(\phi), \dot{\phi} \rangle = -\varepsilon |\nabla V(\phi)|^2 = -\varepsilon \left| \dot{\phi} \right|^2 \leq 0.$$

Furthermore, since the trajectories of (9) are constrained into the  $N$ -dimensional torus  $\mathcal{T}^N$ , which is compact, we are ready to apply LaSalle's invariance principle. Therefore, for every initial condition, the trajectory converges

to the largest invariant set  $M \subset \{\dot{V} \equiv 0\}$ .

Finally, since  $\dot{V}(\phi) \equiv 0$  implies  $|\dot{\phi}| \equiv 0$  we conclude that  $M$  equals the set of all equilibria  $E = \{\phi \in \mathcal{T}^N | \dot{\phi} \equiv 0\} = \bigcup_{\phi^*} E_{\phi^*}$ . So we have proved the following proposition.

**Proposition 1 (Global convergence)** *The dynamics (8) under Assumption 1 converges for every initial condition to the set of equilibrium points  $E$ .* ■

**Remark 2** *Proposition 1 is a generalization of the results of [17] where only the Kuramoto model was considered. Clearly, this is not enough to show almost global stability, since it is possible to have other stable phase-locked equilibria sets besides the in-phase one. However, if we are able show that all the non-in-phase equilibria are unstable, then almost global stability follows. That is the focus of the next section.*

### B. Negative Cut Instability Condition

We now present the main results of this section. Our technique can be viewed as a generalization of [19]. By means of algebraic graph theory, we provide a better stability analysis of the equilibria under a more general framework. We further use the new stability results to characterize  $f_{ij}$  that guarantees almost global stability.

1) *Local Stability Analysis:* Given an equilibrium point  $\phi^*$ , the first order approximation of (9) around  $\phi^*$  is

$$\delta \dot{\phi} = -\varepsilon B \left[ \frac{\partial}{\partial y} F(B^T \phi^*) \right] B^T \delta \phi,$$

were  $\delta \phi = \phi - \phi^*$  is the incremental phase variable, and  $\frac{\partial}{\partial y} F(B^T \phi^*) \in \mathbb{R}^{|E(G)| \times |E(G)|}$  is the Jacobian of  $F(y)$  evaluated at  $B^T \phi^*$ , i.e.,

$$\frac{\partial}{\partial y} F(B^T \phi^*) = \text{diag} (\{f'_{ij}(\phi_j^* - \phi_i^*)\}_{ij \in E(G)}).$$

Now let  $A = -\varepsilon B \left[ \frac{\partial}{\partial y} F(B^T \phi^*) \right] B^T$  and consider the linear system

$$\delta \dot{\phi} = A \delta \phi.$$

Lyapunov's indirect method [30] asserts:

- If there exists an eigenvalue  $\lambda$  of  $A$  with  $\text{Re} \lambda > 0$  then the equilibrium is unstable.

Although it is possible to numerically calculate the eigenvalues of  $A$  given  $\phi^*$ , here we use the special structure of  $A$  to provide a sufficient condition for instability that has nice graph theoretical interpretations.

**Theorem 2 (Negative cut instability condition)** *Given an equilibrium  $\phi^*$  of the system (9), with connectivity graph  $G$  and  $f_{ij}$  satisfying Assumption 1. If there exists a cut  $C(P)$  such that the sum*

$$\sum_{ij \in C(P)} f'_{ij}(\phi_j^* - \phi_i^*) < 0, \quad (10)$$

*the equilibrium  $\phi^*$  is **unstable**.*

*Proof:* Let  $D := \frac{\partial}{\partial y} F(B^T \phi^*)$ . In order to apply the instability criterion of Lyapunov's indirect method, we need to find at least one eigenvalue of  $BDB^T$  with  $\text{Re}\lambda < 0$ . If such eigenvalue existed, it would imply the existence of an eigenvalue of  $A$  with  $\text{Re}\lambda_A > 0$ , and therefore the instability of  $\phi^*$ .

Since  $BDB^T$  is symmetric (recall  $D$  is diagonal), it is enough to find some direction  $x \in \mathcal{V}(G)$  such that  $x^T BDB^T x < 0$ , since that would imply the existence of such negative eigenvalue. Also, since we know that the range of  $B^T$  is the cut space  $\mathcal{C}(G)$ , for any  $y \in \mathcal{C}(G)$  there exists an  $x \in \mathcal{V}(G)$  such that  $y = B^T x$ .

Now let  $y = c_P$  for some partition  $P = (V^-, V^+)$  as defined in (IV-A1) and let  $x_P \in \mathcal{V}(G)$  such that  $c_P = B^T x_P$ . Note that

$$\sum_{ij \in C(P)} f'_{ij}(\phi_j^* - \phi_i^*) = c_P^T D c_P = x_P^T BDB^T x_P.$$

Therefore, when condition (10) holds, there exists some  $x_P \in \mathcal{V}(G)$  with  $x_P^T BDB^T x_P < 0$ , which implies that  $A = -\varepsilon BDB^T$  has at least one eigenvalue whose real part is **positive**. ■

**Remark 3** • *Theorem 2 provides a **sufficient** condition for instability; it is not clear what happens when (10) does not hold. However, it gives a graph-theoretical interpretation that can be used to provide stability results for general topologies. That is, if the **minimum cut cost** is negative, the equilibrium is unstable.*

- *There are several fast algorithms like [31] to find the minimum cut cost of an arbitrary graph that can be used. Thus this Theorem can also provide a computational instability check, alternative to calculating all the eigenvalues of  $A$ , which can be computationally demanding for large networks.*

When (10) is specialized to  $P = (\{i\}, V(G) \setminus \{i\})$  and  $f_{ij}(\theta) = \sin(\theta)$ , it reduces to the instability condition in Lemma 2.3 of [19]; i.e.,

$$\sum_{j \in \mathcal{N}_i} \cos(\phi_j^* - \phi_i^*) < 0. \quad (11)$$

However, (10) has a broader applicability spectrum as the following example shows.

**Example 4** Consider a six oscillators network as in Figure 7, where each node is linked with its four closest neighbors and  $f_{ij}(\theta) = \sin(\theta)$ . Then, by symmetry, it is easy to verify that

$$\phi^* = \left[ 0, \frac{\pi}{3}, \frac{2\pi}{3}, \pi, \frac{4\pi}{3}, \frac{5\pi}{3} \right]^T \quad (12)$$

is an equilibrium of (8).

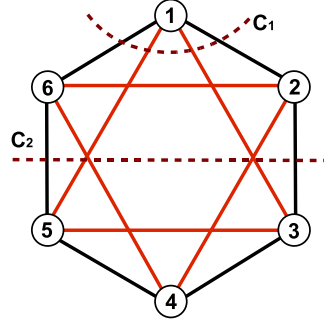


Fig. 7. The network of six oscillators (Example 4)

We first study the stability of  $\phi^*$  using (11) as in [19]. By substituting (12) in  $\cos(\phi_j^* - \phi_i^*) \forall ij \in E(G)$  we find that the edge weights can only take two values:

$$\cos(\phi_j^* - \phi_i^*) = \begin{cases} \cos(\frac{\pi}{3}) = \frac{1}{2}, & \text{if } j = i \pm 1 \pmod{6} \\ \cos(\frac{2\pi}{3}) = -\frac{1}{2}, & \text{if } j = i \pm 2 \pmod{6} \end{cases}$$

Then, since any cut that isolates one node from the rest (like  $C_1 = C(\{1\}, V(G) \setminus \{1\})$  in Figure 7) will always have two edges of each type, their sum is **zero**. Therefore, (11) cannot be used to determine stability.

If we now use Theorem 2 instead, we are allowed to explore a wider variety of cuts that can potentially have smaller costs. In fact, if instead of  $C_1$  we sum over  $C_2 = C(\{1, 2, 6\}, \{3, 4, 5\})$ , we obtain,

$$\sum_{ij \in C_2} \cos(\phi_j^* - \phi_i^*) = -1 < 0,$$

which implies that  $\phi^*$  is unstable.

Figure 8 verifies the equilibrium instability. By starting with an initial condition  $\phi_0 = \phi^* + \delta\phi$  close to the equilibrium  $\phi^*$ , we can see how the system slowly starts to move away from  $\phi^*$  towards a **stable** equilibrium set.

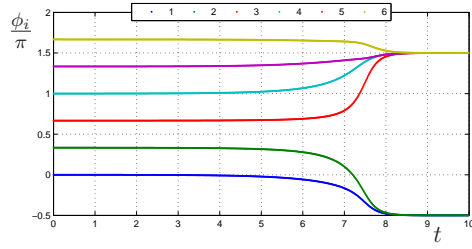


Fig. 8. Unstable equilibrium  $\phi^*$ . Initial condition  $\phi_0 = \phi^* + \delta\phi$

2) *Almost Global Stability*: Condition (10) also provides insight on which class of coupling functions can potentially give us almost global convergence to the in-phase equilibrium set  $E_{1N}$ . If it is possible to find some  $f_{ij}$  with  $f'_{ij}(0) > 0$ , and that for any non-in-phase equilibrium  $\phi^*$ , there is a cut  $C$  with  $\sum_{ij \in C} f'_{ij}(\phi_j^* - \phi_i^*) < 0$ , then the in-phase equilibrium set will be almost globally stable [13]. The main difficulty is that for general  $f_{ij}$  and arbitrary network  $G$ , it is not easy to locate every phase-locked equilibria and thus, it is not simple to know in what region of the domain of  $f_{ij}$  the slope should be negative.

We now concentrate on the one-parameter family of functions  $\mathcal{F}_b$ , with  $b \in (0, \pi)$  defined by:

- Assumption 1
- $f'_{ij}(\theta; b) > 0, \forall \theta \in (0, b) \cup (2\pi - b, 2\pi)$ , and
- $f'_{ij}(\theta; b) < 0, \forall \theta \in (b, 2\pi - b)$ .

See Figure 3 for an illustration with  $b = \frac{3\pi}{4}$ . Also note that this definition implies that if  $f_{ij}(\theta; b) \in \mathcal{F}_b$ , the coupling is attractive and  $f_{ij}(\theta; b) > 0 \forall \theta \in (0, \pi)$ . This last property will be used later.

In order to obtain almost global stability we need  $b$  to be small. However, since the equilibria position is not known a priori, it is not clear how small  $b$  should be or if there is any  $b > 0$  such that all nontrivial equilibria are unstable. We therefore first need to estimate the region of the state space that contains every non-trivial phase-locked solution.

Let  $I$  be a compact connected subset of  $\mathbb{S}^1$  and let  $l(I)$  be its length, e.g., if  $I = \mathbb{S}^1$  then  $l(I) = 2\pi$ . For any  $S \subset V(G)$  and  $\phi \in \mathcal{T}^N$ , define  $I^*(\phi, S)$  as the smallest interval  $I$  such that  $\phi_i \in I \forall i \in S$ , i.e.,

$$I^*(\phi, S) = \underset{I: \phi_i \in I, \forall i \in S}{\operatorname{argmin}} l(I).$$

Since  $S$  is finite and  $I$  is compact,  $I^*$  is always well defined. The extremes of  $I^*$  represent the two phases of  $S$



that are farthest away. Therefore, we can use  $I^*$  to define the separation width of the elements of  $S$  within  $\mathbb{S}^1$  as

$$d(\phi, S) = l(I^*(\phi, S)).$$

Direct application Proposition 2.6 of [16] gives the following Lemma:

**Lemma 3** *Let  $f_{ij}(\cdot; b) \in \mathcal{F}_b \forall ij \in E(G)$  and  $G$  be connected. If  $\phi^*$  is an equilibrium point of (9) and  $d(\phi^*, V(G)) < \pi$ , then it must be the case that  $\phi^*$  is an in-phase equilibrium, i.e.  $\phi^* = \lambda \mathbf{1}_N$  for  $\lambda \in \mathbb{R}$ .*

*Proof:* Suppose  $\phi^*$  is a **non-in-phase** equilibrium with  $d(\phi^*, V(G)) < \pi$ . Then, all the phases are strictly contained in a half circle and for the oscillator with smallest phase  $i_0$ , all the phase differences  $(\phi_j^* - \phi_{i_0}^*) \in (0, \pi)$ . However, since  $f_{ij}(\cdot; b) \in \mathcal{F}_b$  implies  $f_{ij}(\theta; b) > 0 \forall \theta \in (0, \pi)$ ,  $\dot{\phi}_{i_0}^* = \sum_{j \in \mathcal{N}_{i_0}} f_{ij}(\phi_j - \phi_{i_0}) \neq 0$ . Therefore,  $\phi^*$  cannot be an equilibrium which is a contradiction. ■

In other words, there is no equilibria, other than the in-phase one, with all the phases within any given half unit circle. We are now ready to establish a bound on the value of  $b$  that guarantees the instability of the non-in-phase equilibria.

**Lemma 4** *Consider  $f_{ij}(\cdot; b) \in \mathcal{F}_b \forall ij \in E(G)$  and arbitrary connected graph  $G$ . Then for any  $b < \frac{\pi}{N-1}$  and non-in-phase equilibrium  $\phi^*$ , there is a cut  $C$  with*

$$f'_{ij}(\phi_j^* - \phi_i^*; b) < 0, \forall ij \in C$$

*Proof:* Suppose there is a non-in-phase equilibrium  $\phi^*$  for which no such cut  $C$  exists. Let  $V_0^- = \{i_0\}$  and  $V_0^+ = V(G) \setminus \{i_0\}$  be a partition of  $V(G)$  for some arbitrary node  $i_0$ .

Since such  $C$  does not exist, there exists some edge  $i_0 j_1 \in C(V_0^-, V_0^+)$ , with  $j_1 \in V_0^+$ , such that  $f'_{i_0 j_1}(\phi_{j_1}^* - \phi_{i_0}^*; b) \geq 0$ . Move  $j_1$  from  $V_0^+$  to  $V_0^-$  and define  $V_1^- := V_0^- \cup \{j_1\}$  and  $V_1^+ := V_0^+ \setminus \{j_1\}$ . Now since  $f'_{i_0 j_1}(\phi_{j_1}^* - \phi_{i_0}^*; b) \geq 0$ , then

$$d(\phi^*, V_1^-) \leq b.$$

In other words, both phases should be within a distance smaller than  $b$ .

At the  $k^{th}$  iteration, given  $V_{k-1}^-, V_{k-1}^+$ , again we can find some  $i_{k-1} \in V_{k-1}^-, j_k \in V_{k-1}^+$  such that  $i_{k-1} j_k \in C(V_{k-1}^-, V_{k-1}^+)$  and  $f'_{i_{k-1} j_k}(\phi_{j_k}^* - \phi_{i_{k-1}}^*; b) \geq 0$ . Also, since at each step  $d(\phi^*, \{i_{k-1}, j_k\}) \leq b$ ,

$$d(\phi^*, V_k^-) \leq b + d(\phi^*, V_{k-1}^-).$$

Solving the recursion we get:

$$d(\phi^*, V_k^-) \leq kb.$$

Then, after  $N - 1$  iterations we have  $V_{N-1}^- = V(G)$  and  $d(\phi^*, V(G)) < (N - 1)b$ . Therefore, since  $b < \frac{\pi}{N-1}$ , we obtain

$$d(\phi^*, V(G)) < (N - 1)\frac{\pi}{N - 1} = \pi.$$

Then, by Lemma 3  $\phi^*$  must be an in-phase equilibrium, which is a contradiction, since we supposed  $\phi^*$  not to be in-phase. Therefore, for any non-in-phase  $\phi^*$  and  $b < \frac{\pi}{N-1}$ , we can always find a cut  $C$  with  $f_{ij}(\phi_j^* - \phi_i^*; b) < 0$ ,  $\forall ij \in C$ . ■

**Corollary 5** Consider  $f_{ij}(\theta; b) \in \mathcal{F}_b$  and an arbitrary connected graph  $G$ . If  $b < \frac{\pi}{N-1}$ , then any non-in-phase equilibrium  $\phi^*$  is **unstable**.

We now have all the needed elements to prove the following theorem.

**Theorem 6 (Almost global stability)** Consider  $f_{ij}(\theta; b) \in \mathcal{F}_b$  and an arbitrary connected graph  $G$ . Then, if  $b < \frac{\pi}{N-1}$ , the in-phase equilibrium set  $E_{1_N}$  is **almost globally asymptotically stable**.

*Proof:* By Proposition 1, from every initial condition the system (9) converges to the set of equilibria  $E$ . Additionally, since  $b \leq \frac{\pi}{N-1}$ , by Corollary 5 any non-in-phase equilibrium  $\phi^*$  is **unstable**. So the only possible stable solutions are such  $B^T \phi^* = 0$ . Since  $G$  is connected, this only holds when  $\phi^* = \lambda \mathbf{1}_N$  which is always some in-phase equilibrium. Therefore, for almost every initial condition, the system (8) converges to the set of in-phase equilibria  $E_{1_N}$  and thus this set is almost globally asymptotically stable. ■

### C. Complete Graph Topology with a Class of Coupling Functions

In this subsection we investigate how conservative the value of  $b$  found in Section IV-B2 is for the complete graph topology. We are motivated by the results of [19] where it is shown that  $f(\theta) = \sin(\theta)$  ( $b = \frac{\pi}{2}$ ) with complete graph topology ensure almost global synchronization.

Since for general  $f$  it is not easy to characterize all the possible equilibria of the system, we study the stability of the equilibria that appear due to the equivalence of (9) with respect to the action group  $S_N \times T^1$ , where  $S_N$  is the group of permutations of the  $N$  coordinates and  $T^1 = [0, 2\pi)$  represents the group action of phase shift of all the coordinates, i.e. the action of  $\delta \in T^1$  is  $\phi_i \mapsto \phi_i + \delta \forall i$ . We refer the readers to [12] and [16] for a detailed study of the effect of this property.

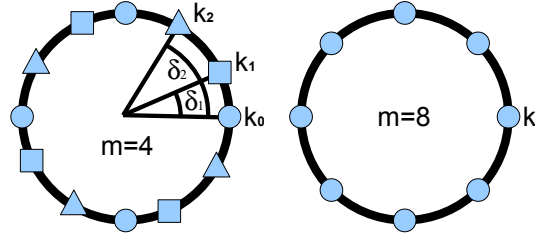


Fig. 9. Equilibria with isotropy  $(S_{k_0} \times S_{k_1} \times S_{k_2})^4 \rtimes Z_4$  (left) and  $(S_k)^8 \rtimes Z_8$  (right)

These equilibria are characterized by the isotropy subgroups  $\Gamma$  of  $S_N \times T^1$  that keeps them fixed, i.e.,  $\gamma\phi^* = \phi^*$   $\forall \gamma \in \Gamma$ . In [12] it was shown that this isotropy subgroup takes the form of

$$(S_{k_0} \times S_{k_1} \times \cdots \times S_{k_{l_B-1}})^m \rtimes Z_m$$

where  $k_i$  and  $m$  are positive integers such that  $(k_0 + k_1 + \cdots + k_{l_B-1})m = N$ ,  $S_j$  is the permutation subgroup of  $S_N$  of  $j$ -many coordinates and  $Z_m$  is the cyclic group with action  $\phi_i \mapsto \phi_i + \frac{2\pi}{m}$ . The semiproduct  $\rtimes$  represents the fact that  $Z_m$  does not commute with the other subgroups.

In other words, each equilibria with isotropy  $(S_{k_0} \times S_{k_1} \times \cdots \times S_{k_{l_B-1}})^m \rtimes Z_m$  is conformed by  $l_B$  shifted constellations  $C_l$  ( $l \in \{0, 1, \dots, l_B - 1\}$ ) of  $m$  evenly distributed blocks, with  $k_l$  oscillators per block. We use  $\delta_l$  to denote the phase shift between constellation  $C_0$  and  $C_l$ . See Figure 9 for examples these types of equilibria.

Here we will show that under mild assumptions on  $f$  and for  $b = \frac{\pi}{2}$  most of the equilibria found with these characteristics are unstable. We first study all the equilibria with  $m$  even. In this case there is a special property, shown in the following lemma, that can be easily exploited.

**Lemma 7** Given  $f \in \mathcal{F}_{\frac{\pi}{2}}$  such that  $f$  is even around  $\frac{\pi}{2}$ , i.e.  $f(\theta - \frac{\pi}{2}) = f(-\theta - \frac{\pi}{2})$ , then for  $m$  **even** the sum

$$g(\delta) = \sum_{j=0}^{m-1} f\left(\frac{2\pi}{m}j + \delta\right) = 0, \quad \forall \delta \in \left[0, \frac{2\pi}{m}\right].$$

*Proof:* The proof of this lemma is a straight consequence of the properties of  $f$  as the next derivation shows.

$$\begin{aligned}
g_m(\delta) &= \sum_{j=0}^{m-1} f\left(\frac{2\pi}{m}j + \delta\right) = \sum_{j=0}^{m/2-1} f\left(\frac{2\pi}{m}j + \delta\right) + f\left(\pi + \frac{2\pi}{m}j + \delta\right) \\
&= \sum_{j=0}^{m/2-1} f\left(\frac{2\pi}{m}j + \delta\right) + f\left(\left(\frac{3\pi}{2} + \frac{2\pi}{m}j + \delta\right) - \frac{\pi}{2}\right) \\
&= \sum_{j=0}^{m/2-1} f\left(\frac{2\pi}{m}j + \delta\right) + f\left(-\left(\frac{2\pi}{m}j + \delta\right)\right) = \sum_{j=0}^{m/2-1} f\left(\frac{2\pi}{m}j + \delta\right) - f\left(\frac{2\pi}{m}j + \delta\right) = 0
\end{aligned}$$

where the third step comes from  $f$  being even around  $\pi/2$  and  $2\pi$ -periodic, and the fourth from  $f$  being odd. ■

Lemma 7 is the key to prove the following instability theorem. It essentially states that the aggregate effect of one constellation  $C_l$  on any oscillator  $j \in V(G) \setminus C_l$  is zero when  $m$  is even, and therefore any perturbation that maintains  $C_l$  has null effect on  $j$ .

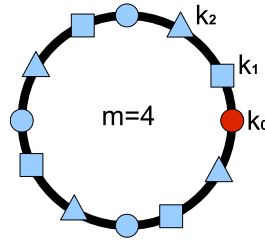


Fig. 10. Cut of Theorem 8, the red block represents one possible set  $V_0$

**Theorem 8 (Instability for even  $m$ )** Given an equilibrium  $\phi^*$  with isotropy  $(S_{k_1} \times S_{k_2} \times \dots \times S_{k_{l_B}})^m \rtimes Z_m$  and  $f \in \mathcal{F}_{\frac{\pi}{2}}$  even around  $\frac{\pi}{2}$ . Then, if  $m$  is even,  $\phi^*$  is unstable.

*Proof:* We will show the instability of  $\phi^*$  by finding a cut of the network satisfying (10). Let  $V_0 \subset V(G)$  be the set of nodes within one of the blocks of the constellation  $C_0$  and consider the partition induced by  $V_0$ , i.e.  $P = (V_0, V(G) \setminus V_0)$ . Due to the structure of  $\phi^*$ , (10) becomes

$$\sum_{ij \in C(P)} f'(\phi_j^* - \phi_i^*) = -k_1 f'(0) + \sum_{l=1}^{l_B} k_l g'_m(\delta_l),$$

where  $g'_m(\delta)$  is the derivative of  $g_m$  as defined in Lemma 7 and  $\delta_l$  is the phase shift between the  $C_0$  and  $C_l$ .

Finally, since by Lemma 7  $g_m(\delta) \equiv 0 \forall \delta$  then it follows that  $g'_m(\delta) \equiv 0$  and

$$\sum_{ij \in C(P)} f'_{ij}(\phi_j^* - \phi_i^*) = -k_1 f'(0) < 0.$$

Therefore, by Theorem 2,  $\phi^*$  is unstable. ■

The natural question that arises is whether similar results can be obtained for  $m$  odd. The main difficulty in this case is that Lemma 7 does not hold since we no longer evaluate  $f$  at points with phase difference equal to  $\pi$  such that they cancel each other. Therefore, an extra monotonicity condition needs to be added in order to partially answer this question. These conditions and their effects are summarized in the following Lemmas.

**Lemma 9 (Monotonicity)** *Given  $f \in \mathcal{F}_{\frac{\pi}{2}}$  such that  $f$  is strictly concave for  $\theta \in [0, \pi]$ , then*

$$f'(\theta) - f'(\theta - \phi) < 0, \quad 0 \leq \theta - \phi < \theta \leq \pi \quad (13)$$

$$f'(\theta) - f'(\theta + \phi) < 0, \quad -\pi \leq \theta < \theta + \phi \leq 0 \quad (14)$$

*Proof:* The proof is a direct consequence of the strict concavity of  $f$ . Since  $f(\theta)$  is strictly concave then basic convex analysis shows that  $f'(\theta)$  is strictly decreasing within  $[0, \pi]$ . Therefore, the inequality (13) follows directly from the fact that  $\theta \in [0, \pi], \theta - \phi \in [0, \pi]$  and  $\theta - \phi < \theta$ . To show (14) it is enough to notice that since  $f$  is odd ( $f \in \mathcal{F}_{\frac{\pi}{2}}$ ),  $f$  is strictly convex in  $[\pi, 2\pi]$ . The rest of the proof is analogous to (13). ■

**Lemma 10 ( $f'$  Concavity)** *Given  $f \in \mathcal{F}_{\frac{\pi}{2}}$  such that  $f'$  is strictly concave for  $\theta \in [-\frac{\pi}{2}, \frac{\pi}{2}]$ . Then for all  $m \geq 4$ ,  $f'(\frac{\pi}{m}) \geq \frac{1}{2}f'(0)$ .*

*Proof:* Since  $f'(\theta)$  is concave for  $\theta \in [-\pi, \pi]$  then it follows

$$f'(\frac{\pi}{m}) = f'(\lambda_m 0 + (1 - \lambda_m)\frac{\pi}{2}) > \lambda_m f'(0) + (1 - \lambda_m)f'(\frac{\pi}{2}) > \lambda_m f'(0)$$

where  $\lambda_m = \frac{m-2}{m}$ . Thus, for  $m \geq 4$ ,  $\lambda_m \geq \frac{1}{2}$  and

$$f'(\frac{\pi}{m}) > \frac{1}{2}f'(0)$$

as desired. ■

Now we show the instability of any equilibria with isotropy  $(S_{k_1} \times S_{k_2} \times \cdots \times S_{k_{i_B}})^m \times Z_m$  for  $m$  odd and greater or equal to 7.

**Theorem 11 (Instability for  $m \geq 7$  and odd)** *Suppose  $f \in \mathcal{F}_{\frac{\pi}{2}}$  with  $f$  concave in  $[0, \pi]$  and  $f'$  concave in*

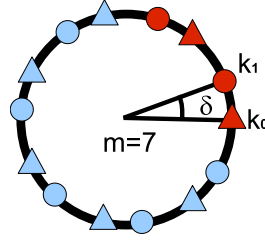


Fig. 11. Cut used in Theorem 11. The dots in red represent all the oscillators of some maximal set  $S$  with  $d(\phi^*, S) < \frac{4\pi}{m}$

$[-\frac{\pi}{2}, \frac{\pi}{2}]$ , then for all  $m = 2k + 1$  with  $k \geq 3$  the equilibria  $\phi^*$ s with isotropy  $(S_{k_1} \times S_{k_2} \times \cdots \times S_{k_{l_B}})^m \rtimes Z_m$  are unstable.

*Proof:* As in Theorem 8 we will use our cut condition to show the instability of  $\phi^*$ . Thus, we define a partition  $P = (S, V(G) \setminus S)$  of  $V(G)$  by taking  $S$  to be a maximal subset of  $V(G)$  such that  $d(\phi, S) < \frac{4\pi}{m}$ , see Figure 11 for an illustration of  $P$ . Notice that any of these partitions will include all the oscillators of two consecutive blocks of every constellation.

Instead of evaluating the total sum of the weights in the cut we will show that the sum of edge weights of the links connecting the nodes of one constellation in  $S$  with the nodes of a possibly different constellation in  $V(G) \setminus S$  is negative. In other words, we will focus on showing

$$\sum_{ij \in \mathcal{K}_{l_1 l_2}} f'(\phi_j^* - \phi_i^*) < 0 \quad (15)$$

where  $\mathcal{K}_{l_1 l_2} = \{ij : i \in C_{l_1} \cap S, j \in C_{l_2} \cap V(G) \setminus S\}$ .

Given any subset of integers  $J$ , we define

$$g_m^J(\delta) = g_m(\delta) - \sum_{j \in J} f\left(\frac{2\pi}{m}j + \delta\right).$$

Then, we can rewrite (15) as

$$\begin{aligned} \sum_{ij \in \mathcal{K}_{l_1 l_2}} f'(\phi_j^* - \phi_i^*) &= (g_m^{\{0,1\}})'(\delta_{l_1 l_2}) + (g_m^{\{-1,0\}})'(\delta_{l_1 l_2}) \\ &= 2g_m'(\delta_{l_1 l_2}) - f'(\delta_{l_1 l_2} + \frac{2\pi}{m}) - 2f'(\delta_{l_1 l_2}) - f'(\delta_{l_1 l_2} - \frac{2\pi}{m}) \end{aligned} \quad (16)$$

where  $\delta_{l_1 l_2} \in [0, \frac{2\pi}{m}]$  is the phase shift between the two constellations. Then, if we can show that for all  $\delta \in [0, \frac{2\pi}{m}]$  (16) is less than zero then for any values of  $l_1$  and  $l_2$  we will have (15) satisfied.

Since  $f$  is odd and even around  $\frac{\pi}{2}$ ,  $f'$  is even and odd around  $\frac{\pi}{2}$  and  $g'_m(\delta)$  can be rewritten as

$$\begin{aligned} g'_m(\delta) &= f'(\delta) \\ &+ \sum_{1 \leq |j| \leq \lfloor \frac{k}{2} \rfloor} \left\{ f'(\delta + \frac{2\pi}{m}j) - f'(\delta - \operatorname{sgn}(j)\frac{\pi}{m} + \frac{2\pi}{m}j) \right\} \\ &- \left[ f'(\delta + \frac{\pi}{m}k) + f'(\delta - \frac{\pi}{m}k) \right] \mathbf{1}_{[k \text{ odd}]} \end{aligned}$$

where  $\mathbf{1}_{[k \text{ odd}]}$  is the indicator function of the event  $[k \text{ odd}]$ , the sum is over all the integers  $j$  with  $1 \leq |j| \leq \lfloor \frac{k}{2} \rfloor$  and  $k = \frac{m-1}{2}$

The last term only appears when  $k$  is odd and in fact it is easy to show that it is always negative as the following calculation shows:

$$\begin{aligned} -f'(\delta + \frac{\pi}{m}k) - f'(\delta - \frac{\pi}{m}k) &= -f'(\frac{\pi}{m}k + \delta) - f'(\frac{\pi}{m}k - \delta) = -f'(\frac{\pi}{2} - \frac{\pi}{2m} + \delta) - f'(\frac{\pi}{2} - \frac{\pi}{2m} - \delta) \\ &= f'(\frac{\pi}{2} - \delta + \frac{\pi}{2m}) - f'(\frac{\pi}{2} - \delta - \frac{\pi}{2m}) = f'(\theta) - f'(\theta - \phi) < 0 \end{aligned}$$

where in step one we used the fact of  $f'$  being even, in step two we used  $k = \frac{m-1}{2}$  and in step three we use  $f'$  being odd around  $\frac{\pi}{2}$ . The last step comes from substituting  $\theta = \frac{\pi}{2} - \delta + \frac{\pi}{2m}$ ,  $\phi = \frac{\pi}{m}$  and apply Lemma 9, since for  $m \geq 7$  we have  $0 \leq \theta - \phi < \theta \leq \pi$ .

Then it remains the show that the terms of the form  $f'(\delta + \frac{2\pi}{m}j) - f'(\delta - \operatorname{sgn}(j)\frac{\pi}{m} + \frac{2\pi}{m}j)$  are negative for all  $j$  s.t.  $1 \leq |j| \leq \lfloor \frac{k}{2} \rfloor$ . This is indeed true when  $j$  is positive since for all  $\delta \in [0, \frac{2\pi}{m}]$  we get

$$0 \leq \delta - \frac{\pi}{m} + \frac{2\pi}{m}j < \delta + \frac{2\pi}{m}j \leq \pi, \text{ for } 1 \leq j \leq \lfloor \frac{k}{2} \rfloor$$

and thus we can apply again Lemma 9.

When  $j$  is negative there is one exception in which Lemma 9 cannot be used since

$$-\pi \leq \delta + \frac{2\pi}{m}j < \delta + \frac{2\pi}{m}j + \frac{\pi}{m} \leq 0, \forall \delta \in [0, \frac{2\pi}{m}]$$

only holds for  $-\lfloor \frac{k}{2} \rfloor \leq j \leq -2$ . Thus the term corresponding to  $j = -1$  cannot be directly eliminated.

Then, by keeping only the terms of the sum with  $j = \pm 1$ ,  $g'_m$  is strictly upper bounded for all  $\delta \in [0, \frac{2\pi}{m}]$  by

$$g'_m(\delta) < f'(\delta) + f'(\delta - \frac{2\pi}{m}) - f'(\delta - \frac{\pi}{m}) + f'(\delta + \frac{2\pi}{m}) - f'(\delta + \frac{\pi}{m}) . \quad (17)$$

Now substituting (17) in (16) we get

$$\begin{aligned} \sum_{ij \in \mathcal{K}_{l_1 l_2}} f'(\phi_j^* - \phi_i^*) &< f'(\delta - \frac{2\pi}{m}) - 2f'(\delta - \frac{\pi}{m}) + f'(\delta + \frac{2\pi}{m}) - 2f'(\delta + \frac{\pi}{m}) \\ &\leq f'(\delta - \frac{2\pi}{m}) - 2f'(\delta - \frac{\pi}{m}) - f'(\delta + \frac{\pi}{m}) \leq f'(\delta - \frac{2\pi}{m}) - 2f'(\delta - \frac{\pi}{m}) \end{aligned}$$

where in the last step we used the fact that for  $m \geq 6$  and  $\delta \in [0, \frac{2\pi}{m}]$ ,  $f'(\delta + \frac{\pi}{m}) \geq 0$ .

Finally, since for  $\delta \in [0, \frac{2\pi}{m}]$   $f'(\delta - \frac{2\pi}{m})$  is strictly increasing and  $f'(\delta - \frac{\pi}{m})$  achieves its minimum for  $\delta \in \{0, \frac{2\pi}{m}\}$ , then

$$f'(\delta - \frac{2\pi}{m}) - 2f'(\delta - \frac{\pi}{m}) \leq f'(0) - 2f'(\frac{\pi}{m}) \leq 0$$

where the last inequality follow from Lemma 10.

Therefore, for all  $m$  odd greater or equal to 7 we obtain

$$\sum_{ij \in \mathcal{K}_{l_1 l_2}} f'(\phi_j^* - \phi_i^*) < f'(0) - 2f'(\frac{\pi}{m}) \leq 0$$

and since this result is independent on the indices  $l_1, l_2$ , then

$$\sum_{ij \in C(S, V(G) \setminus S)} f'(\phi_j^* - \phi_i^*) = \sum_{l_1=1}^{l_B} \sum_{l_2=1}^{l_B} \sum_{ij \in \mathcal{K}_{l_1 l_2}} f'(\phi_j^* - \phi_i^*) < 0$$

and  $\phi^*$  is unstable. ■

## V. EFFECT OF DELAY

Once delay is introduced to the system of coupled oscillators, the problem becomes fundamentally harder. For example, for pulse-coupled oscillators, the reception of a pulse no longer gives accurate information about the relative phase difference  $\Delta\phi_{ij} = \phi_j - \phi_i$  between the two interacting oscillators. Before, at the exact moment when  $i$  received a pulse from  $j$ ,  $\phi_j$  was zero and the phase difference was estimated locally by  $i$  as  $\Delta\phi_{ij} = -\phi_i$ . However, now when  $i$  receives the pulse, the difference becomes  $\Delta\phi_{ij} = -\phi_i - \psi_{ij}$ . Therefore, the delay propagation acts as an error introduced to the phase difference measurement and unless some information is known about this error, it is not possible to predict the behavior. Moreover, as we will see later, slight change in the distribution can produce nonintuitive behaviors. Even though it may not be satisfactory for some applications, many existing works choose to ignore delay. (see for e.g., [22], [18], [19], [26]). That is mainly for analytical tractability.

In this section we study how delay affects the dynamics of a network of pulse-coupled oscillators. A new



framework to study pulse-coupled oscillators with delay will be set up by constructing an equivalent non-delayed system that has the same behavior as the original one in the continuum limit. We then further use this result to show that heterogeneous delay can help reach synchronization, which is a bit counterintuitive and significantly generalizes previous related studies [21], [32], [33]. We will assume complete graph to simplify notation and exposition although the results can be extended for a boarder class of densely connected networks.

We first generalize the intuition from Example 3 in section III to a network of large numbers of oscillators. This is a challenging task given the heterogeneous delay. We shall build on existing arguments such as mean field approximation [25] and Lyapunov stability theory [19], [17] while looking at the problem from a different perspective.

Consider the case where the coupling between oscillators is all to all and identical ( $\mathcal{N}_i = \mathcal{N} \setminus \{i\}$ ,  $\forall i \in \mathcal{N}$  and  $f_{ij} = f \forall i, j$ ). And assume the phase lags  $\psi_{ij}$  are randomly and independently chosen from the same distribution with probability density  $g(\psi)$ . By letting  $N \rightarrow +\infty$  and  $\varepsilon \rightarrow 0$  while keeping  $\varepsilon N =: \bar{\varepsilon}$  a constant, (3) becomes

$$v(\phi, t) := \omega + \bar{\varepsilon} \int_{-\pi}^{\pi} \int_0^{+\infty} f(\sigma - \phi - \psi) g(\psi) \rho(\sigma, t) d\psi d\sigma, \quad (18)$$

where  $\rho(\phi, t)$  is a time-variant normalized phase distribution that keeps track of the fraction of oscillators with phase  $\phi$  at time  $t$ , and  $v(\phi, t)$  is the velocity field that expresses the net force that the whole population applies to a given oscillator with phase  $\phi$  at time  $t$ . Since the number of oscillators is preserved at any time, the evolution of  $\rho(\phi, t)$  is governed by the continuity equation

$$\frac{\partial \rho}{\partial t} + \frac{\partial}{\partial \phi}(\rho v) = 0 \quad (19)$$

with the boundary conditions  $\rho(0, t) \equiv \rho(2\pi, t)$ .

Equations (18)-(19) are not analytically solvable in general. Here we propose a new perspective that is inspired by the following observation.

**Theorem 12** *Mean Field Approximation*

*Let  $\psi_{ij}$  be independent and identically distributed random variables with probability density function  $g(\psi)$ . Then, there is a non-delayed system of the form*

$$\dot{\phi}_i = \omega + \varepsilon \sum_{j \in \mathcal{N}_i} H(\phi_j - \phi_i), \quad (20)$$

where

$$H(\theta) = f * g(\theta) = \int_0^{+\infty} f(\theta - \psi)g(\psi)d\psi \quad (21)$$

is the convolution between  $f$  and  $g$  such that (3) and (20) have the same continuum limit.

*Proof:* By the same reasoning of (18) it is easy to see that the limiting velocity field of (20) is

$$\begin{aligned} v_H(\phi, t) &= \omega + \bar{\varepsilon} \int_0^{2\pi} H(\sigma - \phi)\rho(\sigma, t)d\sigma \\ &= \omega + \bar{\varepsilon} \int_0^{2\pi} \left( \int_0^{+\infty} f((\sigma - \phi) - \psi)g(\psi)d\psi \right) \rho(\sigma, t)d\sigma \\ &= \omega + \bar{\varepsilon} \int_0^{2\pi} \int_0^{+\infty} f(\sigma - \phi - \psi)g(\psi)\rho(\sigma, t)d\psi d\sigma = v(\phi, t) \end{aligned}$$

where in the first and the third steps we used (21) and (18) respectively. Thus both systems produce the same velocity field in the limit and therefore behave identically. ■

**Remark 4** Although (20) is quite different from (3), Theorem 12 states that both systems behave exactly the same in the continuum limit. Therefore, as  $N$  grows, (20) starts to become a good approximation of (3) and therefore can be analyzed to understand the behavior of (3).

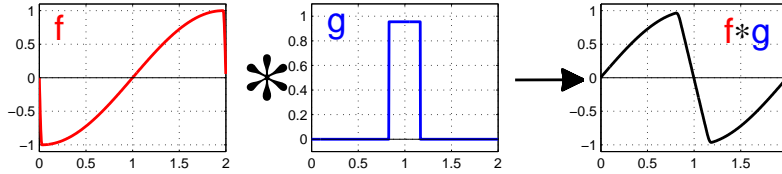


Fig. 12. Effect of delay in coupling shape

Figure 12 shows how, as in the case of two oscillators, the underlying delay (in this case the delay distribution) determines what type of coupling (attractive or repulsive) produces synchronization. The original function  $f$  produces repulsive coupling, whereas the corresponding  $H$  is attractive. In fact, as we will soon see, the distribution of delay not only can qualitatively affect the type of coupling but also can change the stability of certain phase-locked limit cycles.

We now study two example to illustrate how this new approximation can provide significant information about performance and stability of the original system. We also provide numerical simulations to verify our predictions.

### A. Kuramoto Model

We start by studying an example in the literature [34] to demonstrate how we can use the previous equivalent non-delayed formulation to provide a better understanding of systems of pulse-coupled oscillators with delay. When  $f(\theta) = K \sin(\theta)$ ,  $H(\theta)$  can be easily calculated:

$$\begin{aligned} H(\theta) &= \int_0^{+\infty} K \sin(\theta - \psi) g(\psi) d\psi = K \int_0^{+\infty} \Im \left[ e^{i(\theta - \psi)} g(\psi) \right] d\psi \\ &= K \Im \left[ e^{i\theta} \int_0^{+\infty} e^{-i\psi} g(\psi) d\psi \right] = K \Im \left[ e^{i\theta} C e^{-i\xi} \right] = KC \sin(\theta - \xi) \end{aligned}$$

where  $\Im$  is the imaginary part of a complex number, i.e.  $\Im[a + ib] = b$ . The values of  $C > 0$  and  $\xi$  are calculated using the identity

$$C e^{i\xi} = \int_0^{+\infty} e^{i\psi} g(\psi) d\psi.$$

This complex number, usually called ‘‘order parameter’’, provides a measure of how the phase-lags are distributed within the unit circle. It can also be interpreted as the center of mass of the lags  $\psi_{ij}$ ’s when they are thought of as points ( $e^{i\psi_{ij}}$ ) within the unit circle  $\mathbb{S}^1$ . Thus, when  $C \approx 1$ , the  $\psi_{ij}$ ’s are mostly concentrated around  $\xi$ . When  $C \approx 0$ , the delay is distributed such that  $\sum_{ij} e^{i\psi_{ij}} \approx 0$ .

In this example, (20) becomes

$$\dot{\phi}_i = \omega + \varepsilon KC \sum_{j \in \mathcal{N}_i} \sin(\phi_j - \phi_i - \xi). \quad (22)$$

Here we see how the distribution of  $g(\psi)$  has a direct effect on the dynamics. For example, when the delays are heterogeneous enough such that  $C \approx 0$ , the coupling term disappears and therefore makes synchronization impossible. A complete study of the system under the context of superconducting Josephson arrays was performed [34] for the complete graph topology. There the authors characterized the condition for in-phase synchronization in terms of  $K$  and  $C e^{i\xi}$ . More precisely, when  $K C e^{i\xi}$  is on the right half of the plane ( $K C \cos(\xi) > 0$ ), the system almost always synchronizes. However, when  $K C e^{i\xi}$  is on the left half of the plane ( $K C \cos(\xi) < 0$ ), the system moves towards an incoherent state where all of the oscillators’ phases spread around the unit circle such that its order parameter, i.e.  $\frac{1}{N} \sum_{l=1}^N e^{i\phi_l}$ , becomes zero.

Another way to interpret the parameter  $\xi$  is as if every signal were delayed by the same amount. Then the previous conditions are akin to the ones discussed for two oscillator with delay, where we showed that if  $\xi = \pi$  ( $\cos(\xi) = -1$ ) then  $K < 0$  (repulsive coupling) produces synchronization, whereas when  $\xi = 0$  ( $\cos(\xi) = 1$ ),  $K > 0$  is the one that synchronizes.

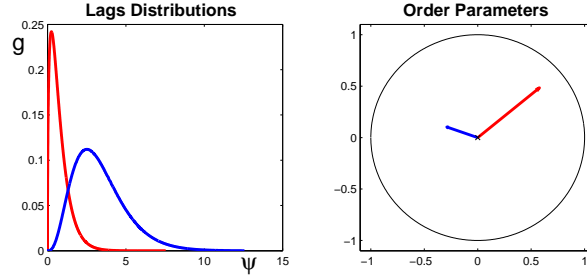


Fig. 13. Delay distributions and their order parameter  $Ce^{i\xi}$

We now provide simulation results to illustrate how (22) becomes a good approximation of the original system when  $N$  is large enough. We simulate the original repulsive ( $K < 0$ ) sine-coupled system with heterogeneous delays and its corresponding approximation (22). Two different delay distributions, depicted in Figure 13, were selected such that their corresponding order parameter lie in different half-planes.

The same simulation is repeated for  $N = 5, 10, 50$ . Figure 14 shows that when  $N$  is small, the phases' order parameter of the original system (in red/blue) draw a trajectory which is completely different with respect to its approximation (in green). However, as  $N$  grows, in both cases the trajectories become closer and closer. Since  $K < 0$ , the trajectory of the system with wider distribution ( $C \cos \xi < 0$ ) drives the order parameter towards the boundary of the circle, i.e., **heterogeneous delay leads to homogeneous phase**.

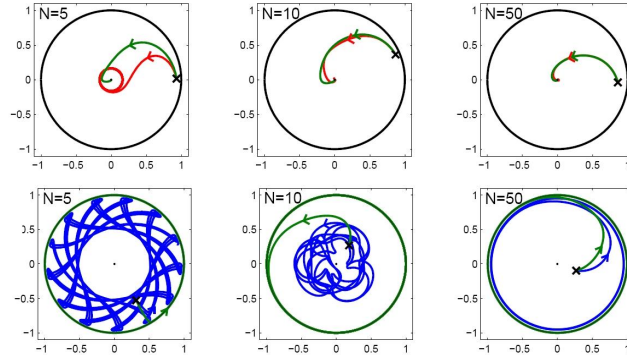


Fig. 14. Repulsive sine coupling with heterogeneous delays

### B. Effect of Heterogeneity

We now explain a more subtle effect that heterogeneity can produce. Consider the system in (20) where  $H$  after the convolution falls under Assumption 1. Then, from Section IV, all of the oscillators eventually end up running at the same speed  $\omega$  with fixed phase difference such that the sum  $\sum_{i \in \mathcal{N}_i} H(\phi_j - \phi_i)$  cancels  $\forall i$ .

Moreover, we can apply Theorem 2 to assess the stability of these orbits. Therefore, if we can find a cut  $\mathcal{K}$  of the network such that  $\sum_{ij \in \mathcal{K}} H'(\phi_j^* - \phi_i^*) < 0$ , the phase-locked solution will be unstable.

Although this condition is for non-delayed phase-coupled oscillators, the result of this section allows us to translate it for systems with delay. Since  $H$  is the convolution of the coupling function  $f$  and the delay distribution function  $g$ , we can obtain  $H'(\phi_j^* - \phi_i^*) < 0$ , even when  $f'(\phi_j^* - \phi_i^*) > 0$ . This usually occurs when the convolution widens the region with a negative slope of  $H$ . See Figure 12 for an illustration of this phenomenon.

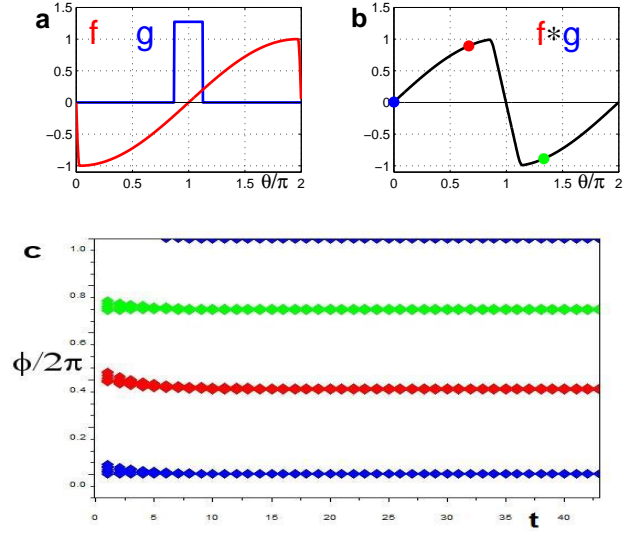


Fig. 15. Pulse-coupled oscillators with delay: Stable equilibrium

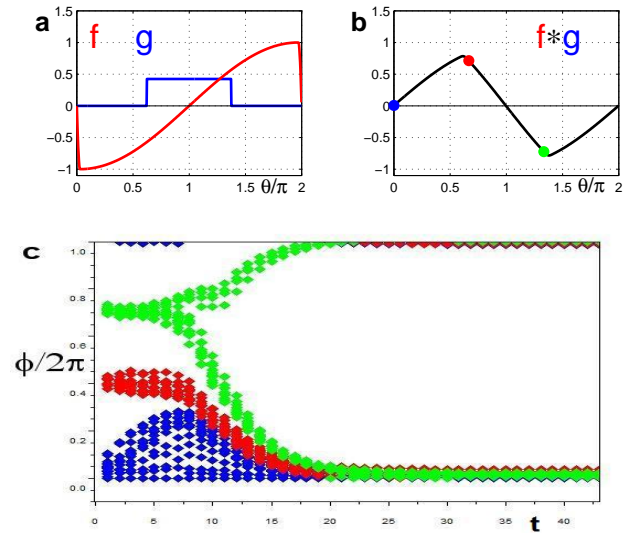


Fig. 16. Pulse-coupled oscillators with delay: Unstable equilibrium

Figures 15 and 16 show two simulation setups of 45 oscillators pulse-coupled all to all. The initial state is close to a phase locked configuration formed of three equidistant clusters of 15 oscillators each. The shape of the coupling function  $f$  and the phase lags distributions are shown in part a; while  $f$  is maintained unchanged between both simulations, the distribution  $g$  does change. Thus, the corresponding  $H = f * g$  changes as it can be seen in part b; the blue, red, and green dots correspond to the speed change induced in an oscillator within the blue cluster by oscillators of each cluster. Since all clusters have the same number of oscillators, the net effect is zero. In part c the time evolution of oscillators' phases relative to the phase of a blue cluster oscillator are shown. Although the initial conditions are exactly the same, the wider delay distribution on Figure 16 produces negative slope on the red and green points of part b, which destabilizes the clusters and drives oscillators toward in-phase synchrony.

Finally, we simulate the same scenario as in Figures 15 and 16 but now changing  $N$  and the standard deviation, i.e. the delay distribution width. Figure 17 shows the computation of the synchronization probability vs. standard deviation. The dashed line denotes the minimum value that destabilizes the equivalent system. As  $N$  grows, the distribution shape becomes closer to a step, which is the expected shape in the limit. It is quite surprising that as soon as the equilibrium is within the region of  $H$  with negative slope, the equilibrium becomes unstable as the theory predicts.

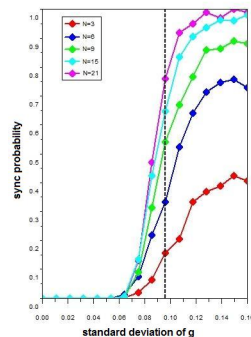


Fig. 17. **Pulse-coupled oscillators with delay: Synchronization probability**

## VI. CONCLUSION

This paper analyzes the dynamics of identical weakly coupled oscillators while relaxing several classical assumptions on coupling, delay and topology. Our results provide global synchronization guarantee for a wide

range of scenarios. There are many directions that can be taken to further this study. For example, for different topologies, to guarantee global in-phase synchronization, how does the requirement on coupling functions change? Another specific question is to complete the proof in Section IV-C for the cases when  $m = 1, 3, 5$ . Finally, it will be of great interest if we can apply results and techniques in this paper to a wide range of applications such as transient stability analysis of power networks and clock synchronization of computer networks.

**Acknowledgments:** The authors thank S. Strogatz of Cornell for useful discussions.

## REFERENCES

- [1] A. T. Winfree, "Biological rhythms and the behavior of populations of coupled oscillators," *Journal of Theoretical Biology*, vol. 16, no. 1, pp. 15 – 42, 1967.
- [2] C. S. Peskin, *Mathematical aspects of heart physiology*. New York, NY, USA: Courant Institute of Mathematical Sciences, New York University, 1975.
- [3] P. Achermann and H. Kunz, "Modeling circadian rhythm generation in the suprachiasmatic nucleus with locally coupled self-sustained oscillators: Phase shifts and phase response curves," *Journal of Biological Rhythms*, vol. 14, no. 6, pp. 460 – 468, 1999.
- [4] J. Garcia-Ojalvo, M. B. Elowitz, S. H. Strogatz, and C. S. Peskin, "Modeling a synthetic multicellular clock: Repressilators coupled by quorum sensing," *Proceedings of the National Academy of Sciences of the United States of America*, vol. 101, no. 30, pp. 10955–10960, 2004.
- [5] S. Yamaguchi, H. Isejima, T. Matsuo, R. Okura, K. Yagita, M. Kobayashi, and H. Okamura, "Synchronization of cellular clocks in the suprachiasmatic nucleus," *Science*, vol. 32, pp. 1408–1412, Nov. 2003.
- [6] I. Z. Kiss, Y. Zhai, and J. L. Hudson, "Emerging coherence in a population of chemical oscillators," *Science*, vol. 296, pp. 1676–1678, Nov. 2002.
- [7] R. York and R. Compton, "Quasi-optical power combining using mutually synchronized oscillator arrays," *IEEE Transactions on Microwave Theory and Techniques*, vol. 39, pp. 1000–1009, Jun. 1991.
- [8] Y.-W. Hong and A. Scaglione, "A scalable synchronization protocol for large scale sensor networks and its applications," *IEEE Journal on Selected Areas in Communications*, vol. 23, pp. 1085–1099, May. 2005.
- [9] G. Werner-Allen, G. Tewari, A. Patel, M. Welsh, and R. Nagpal, "Firefly-inspired sensor network synchronicity with realistic radio effects," in *SenSys: Proceedings of the 3rd International Conference on Embedded Networked Sensor Systems*, (New York, NY, USA), pp. 142–153, ACM, 2005.
- [10] S. A. Marvel and S. H. Strogatz, "Invariant submanifold for series arrays of josephson junctions," *Chaos*, vol. 19, p. 013132, Mar. 2009.
- [11] P. C. Bressloff and S. Coombes, "Travelling waves in chains of pulse-coupled integrate-and-fire oscillators with distributed delays," *Phys. D*, vol. 130, no. 3-4, pp. 232–254, 1999.
- [12] P. Ashwin and J. W. Swift, "The dynamics of n weakly coupled identical oscillators," *J. Nonlinear Sci*, vol. 2, no. 1, pp. 69–108, 1992.
- [13] G. B. Ermentrout, "Stable periodic solutions to discrete and continuum arrays of weakly coupled nonlinear oscillators," *SIAM J. Appl. Math.*, vol. 52, no. 6, pp. 1665–1687, 1992.

- [14] Y. Kuramoto, “International symposium on mathematical problems in theoretical physics,” in *Lecture notes in Physics*, vol. 39, p. 420, Springer, 1975.
- [15] O. V. Popovych, Y. L. Maistrenko, and P. A. Tass, “Phase chaos in coupled oscillators,” *Phys. Rev. E*, vol. 71, p. 065201, Jun. 2005.
- [16] E. Brown, P. Holmes, and J. Moehlis, “Globally coupled oscillator networks,” in *Perspectives and Problems in Nonlinear Science: A Celebratory Volume in Honor of Larry Sirovich*, pp. 183–215, Springer, 2003.
- [17] A. Jadbabaie, N. Motee, and M. Barahona, “On the stability of the kuramoto model of coupled nonlinear oscillators,” in *Proceedings of the American Control Conference.*, vol. 5, pp. 4296–4301, June 30, 2004.
- [18] D. Lucarelli and I.-J. Wang, “Decentralized synchronization protocols with nearest neighbor communication,” in *Proceedings of the 2nd International Conference on Embedded Networked Sensor Systems*, 2004.
- [19] P. Monzón and F. Paganini, “Global considerations on the kuramoto model of sinusoidally coupled oscillators,” in *Proceedings of the 44th IEEE Conference on Decision and Control, and European Control Conference*, (Sevilla, Spain), pp. 3923–3928, Dec. 2005.
- [20] E. M. Izhikevich, “Phase models with explicit time delays,” *Phys. Rev. E*, vol. 58, pp. 905–908, Jul. 1998.
- [21] E. M. Izhikevich, “Weakly pulse-coupled oscillators, fm interactions, synchronization, and oscillatory associative memory,” *IEEE Transactions on Neural Networks*, vol. 10, pp. 508–526, May. 1999.
- [22] R. E. Mirollo and S. H. Strogatz, “Synchronization of pulse-coupled biological oscillators,” *SIAM J. Appl. Math.*, vol. 50, pp. 1645–1662, 1990.
- [23] U. Ernst, K. Pawelzik, and T. Geisel, “Synchronization induced by temporal delays in pulse-coupled oscillators,” *Phys. Rev. Lett.*, vol. 74, pp. 1570–1573, Feb. 1995.
- [24] U. Ernst, K. Pawelzik, and T. Geisel, “Delay-induced multistable synchronization of biological oscillators,” *Phys. Rev. E*, vol. 57, pp. 2150–2162, Feb. 1998.
- [25] Y. Kuramoto, *Chemical Oscillations, Waves, and Turbulence*. Berlin Heidelberg New York Tokyo: Springer-Verlag, 1984.
- [26] A. Papachristodoulou and A. Jadbabaie, “Synchronization in oscillator networks with heterogeneous delays, switching topologies and nonlinear dynamics,” in *Proceedings of the 45th IEEE Conference on Decision and Control*, pp. 4307–4312, Dec. 2006.
- [27] A. Rantzer, “A dual to lyapunov’s stability theorem,” *Systems and Control Letters*, vol. 42, pp. 161–168, 2001.
- [28] B. Bollobas, *Modern Graph Theory*. New York: Springer, 1998.
- [29] C. Godsil and G. Royle, *Algebraic Graph Theory*. New York: Springer, 2001.
- [30] H. K. Khalil, *Nonlinear systems; 3rd ed.* Prentice-Hall, 1996.
- [31] S. Xu, “The line index and minimum cut of weighted graphs,” *European Journal of Operational Research*, vol. 109, pp. 672–685, Sep. 1998.
- [32] C. van Vreeswijk, L. Abbott, and G. B. Ermentrout, “When inhibition not excitation synchronizes neural firing,” *Journal of Computational Neuroscience*, vol. 1, no. 4, pp. 313–321, 1994.
- [33] W. Gerstner, “Rapid phase locking in systems of pulse-coupled oscillators with delays,” *Phys. Rev. Lett.*, vol. 76, pp. 1755–1758, Mar 1996.
- [34] S. Watanabe and S. H. Strogatz, “Constants of motion for superconducting josephson arrays,” *Phys. D*, vol. 74, no. 3-4, pp. 197–253, 1994.